Plant and Cell Physiology Advance Access published March 27, 2015

PCP
PLANT & CELL PHYSIOLOGY

Base to Tip and Long-Distance Transport of Sodium in the Root of Common Reed [*Phragmites australis* (Cav.) Trin. ex Steud.] at Steady State Under Constant High-Salt Conditions

Shu Fujimaki[1], Teppei Maruyama[2], Nobuo Suzui[1], Naoki Kawachi[1], Eitaro Miwa[2] and Kyoko Higuchi[2,*]

[1]Quantum Beam Science Center, Japan Atomic Energy Agency, 1233 Watanuki, Takasaki, Gunma, 370-1292 Japan
[2]Laboratory of Plant Production Chemistry, Department of Applied Biology and Chemistry, Tokyo University of Agriculture, 1-1-1 Sakuragaoka, Setagaya, Tokyo, 156-8502 Japan
*Corresponding author: E-mail, khiguchi@nodai.ac.jp; Fax, +81-354772315.
(Received April 17, 2014; Accepted February 3, 2015)

We analyzed the directions and rates of translocation of sodium ions (Na^+) within tissues of a salt-tolerant plant, common reed [*Phragmites australis* (Cav.) Trin. ex Steud.], and a salt-sensitive plant, rice (*Oryza sativa* L.), under constant high-salt conditions using radioactive ^{22}Na tracer and a positron-emitting tracer imaging system (PETIS). First, the test plants were incubated in a nutrient solution containing 50 mM NaCl and a trace level of ^{22}Na for 24 h (feeding step). Then the original solution was replaced with a fresh solution containing 50 mM NaCl but no ^{22}Na, in which the test plants remained for >48 h (chase step). Non-invasive dynamic visualization of ^{22}Na distribution in the test plants was conducted during feeding and chase steps with PETIS. Our results revealed that ^{22}Na was absorbed in the roots of common reed, but not transported to the upper shoot beyond the shoot base. During the chase step, a basal to distal movement of ^{22}Na was detected within the root tissue over >5 cm with a velocity of approximately 0.5 cm h^{-1}. On the other hand, ^{22}Na that was absorbed in the roots of rice was continuously translocated to and accumulated in the whole shoot. We concluded that the basal roots and the shoot base of common reed have constitutive functions of Na^+ exclusion only in the direction of root tips, even under constant high-salt conditions. This function apparently may contribute to the low Na^+ concentration in the upper shoot and high salt tolerance of common reed.

Keywords: Common reed • Na • PETIS • Phloem • Salt tolerance • Xylem.

Abbreviations: PETIS, positron-emitting tracer imaging system; ROI, region of interest; SB, shoot base.

Introduction

Higher plants have various mechanisms of tolerance to sodium ions (Na^+). Na^+ has a detrimental effect on the growth of most plants belonging to the glycophytes. In temperate regions, the Na^+ concentration in the soil solution is on average 0.1–1 mM (similar to the K^+ concentration), and reaches >50 mM in semi-arid and arid regions (Marschner 1995). The exclusion of Na^+ from the upper shoot, including the photosynthetic organs, is considered important for Na^+ tolerance, especially in gramineous plants, and their mechanisms for Na^+ exclusion have been intensively investigated (Møller and Tester 2007). Physiological approaches have revealed that Na^+ that has penetrated into the shoot via xylem vessels or apoplast can be retrieved and retranslocated via the phloem and then excluded from photosynthetic organs (Wolf et al. 1990, Lohaus et al. 2000). The radioisotope ^{22}Na has been used to study Na^+ translocation within plant tissues. For example, James et al. (2006) reported that Na^+ export from the shoot was only a small proportion of the import to the shoot (probably not more than 10%) in a durum wheat line which has low Na^+ concentrations in leaf blades. Using a split-root system, Kong et al. (2012) demonstrated that Na^+ absorbed into one bundle of cotton roots was translocated to and excreted from the other bundle, but the sites of Na^+ retrieval from the xylem and Na^+ loading into the phloem in the shoot, and the rate of Na^+ retranslocation, are still not clear.

Recent developments in molecular biology have resulted in identification of many Na^+ transporters and analysis of Na^+ exclusion. In particular, SOS1 and HKT are important for Na^+ exclusion from plants. SOS1 regulates Na^+ concentration in the xylem sap in *Arabidopsis thaliana* (Shi et al. 2003) and tomato (*Solanum lycopersicum* L.) (Olías et al. 2009). Class I HKT contributes to Na^+ retrieval from the xylem sap (Ren et al. 2005, Sunarpi et al. 2005, Huang et al. 2008, Munns et al. 2012); however, the destination of retrieved Na^+ is still unclear (Horie et al. 2009). The retrieval of Na^+ at the basal part of the roots was suggested by the results of the experiments that used an *HKT* knockout mutant of Arabidopsis with only one copy of the *HKT* gene. However, this AtHKT1;1 may not be involved in the recirculation of the phloem (Davenport et al. 2007). These studies have suggested that the retranslocation of Na^+ from the shoot to the roots takes place through the phloem. However, these conclusions were based on the balance of Na^+ influx and efflux, but not on any direct observations of Na^+ movement.

Under high-salt conditions, an Na^+-tolerant gramineous plant, common reed [*Phragmites australis* (Cav.) Trin. ex Steud.], has a very low concentration of Na^+ in the shoot but not in the roots in comparison with Na^+-sensitive rice (*Oryza*

Plant Cell Physiol. 0(0): 1–8 doi:10.1093/pcp/pcv021, Advance Access publication on 8 February 2015, available online at www.pcp.oxfordjournals.org

sativa L.) (Matsushita and Matoh 1991). We previously reported that the Na^+ concentration in the xylem sap was lower in the shoot base than in the roots of common reed (Kanai et al. 2007). This result suggested that common reed has the ability to retrieve Na^+ efficiently from the xylem before it enters the shoot region, not simply to exclude it from the root epidermis or cortex; as a consequence, translocation of Na^+ from roots to shoots is strongly suppressed in this species. Class II HKT and SOS1 have been identified in common reed (Takahashi et al. 2007, Takahashi et al. 2009) but their contribution to Na^+ retrieval from the xylem is still unknown. Active retranslocation of Na^+ from the shoot to the roots via the phloem in common reed has been suggested: a short feeding of ^{22}Na to the root and inactivation of the phloem function at the shoot base by heat-girdling increased ^{22}Na abundance in the upper shoot (Matsushita and Matoh 1992). However, direct observations of the movement of Na^+ in common reed are also required to elucidate the total mechanism.

Only a limited number of experimental techniques are suitable for direct demonstration of solute movement in the root phloem. Chemical analysis of phloem sap in the root is very difficult because collection of pure phloem sap by insect stylectomy is only applicable to the shoot. The split-root system has been employed only for detection of Na^+ efflux into low-Na^+ solutions from roots after absorption by the other half of the root system immersed in a high-Na^+ solution (Blom-Zandstra et al. 1998, Kong et al. 2012). Therefore, the existence of backward transport of Na^+ against the gradient of Na^+ concentration as a potential constitutive function necessary for Na^+ tolerance cannot be concluded with certainty by using the split-root system. In addition, it is not applicable for analysis of the bidirectional transport within the same root.

In this study, we employed a positron-emitting tracer imaging system (PETIS), a non-invasive imaging technique for positron-emitting radiotracers (including ^{22}Na) with a fine spatial resolution (a few millimeters) (Uchida et al. 2004), which can trace the changes in distribution of the substance of interest (reviewed in Fujimaki et al. 2010). The key idea is that the natural movement of Na^+ in a plant body can be traced by using this technique even after Na^+ influx and efflux reach equilibrium under continuous and constant high-Na^+ conditions if very small amounts of ^{22}Na are fed to the plant for a short period at the beginning of the observation (pulse–chase experiments). This approach enables quantitative and time course analyses of absorption, transport and excretion of Na^+ under the continuous presence of Na^+. In this study, we analyzed and compared the directions of ^{22}Na movement in common reed and rice using PETIS to understand the mechanisms of Na^+ transport within the root and shoot after absorption.

Results

Dynamic images of ^{22}Na movement in plant bodies

The common reed plants and rice plants were incubated in hydroponic culture solution containing 50 mM non-radioactive NaCl and a trace level of ^{22}Na for 24 h (feeding step), and the original solution was replaced by a fresh one containing only non-radioactive 50 mM NaCl but no ^{22}Na, then the plants were incubated for >48 h (chase step) (**Fig. 1**). Note that 50 mM non-radioactive Na^+ was constantly present in the nutrient solution throughout the experiment, and the increase in total Na^+ concentration due to addition of ^{22}Na was negligible. We confirmed in advance that the shoot dry weight of neither common reed nor rice was significantly affected by salt stress during the experimental period (**Supplementary Fig. S1**), and thus we considered that 50 mM NaCl is below the harmful level for these two species. The amount of ^{22}Na absorbed by the test plants was calculated by summation of radioactivity in the whole shoot including the shoot base, the root and the nutrient solution after the chase step (**Fig. 2**). The effect of a 3 d 50 mM NaCl acclimation pre-treatment on the absorption and partitioning of ^{22}Na was examined; no significant differences were found in the absorption of ^{22}Na for any of the two species, although a decreasing tendency was observed. In rice, the distribution ratio in the shoot was significantly reduced, while in the nutrient solution it was significantly increased (**Fig. 2B**).

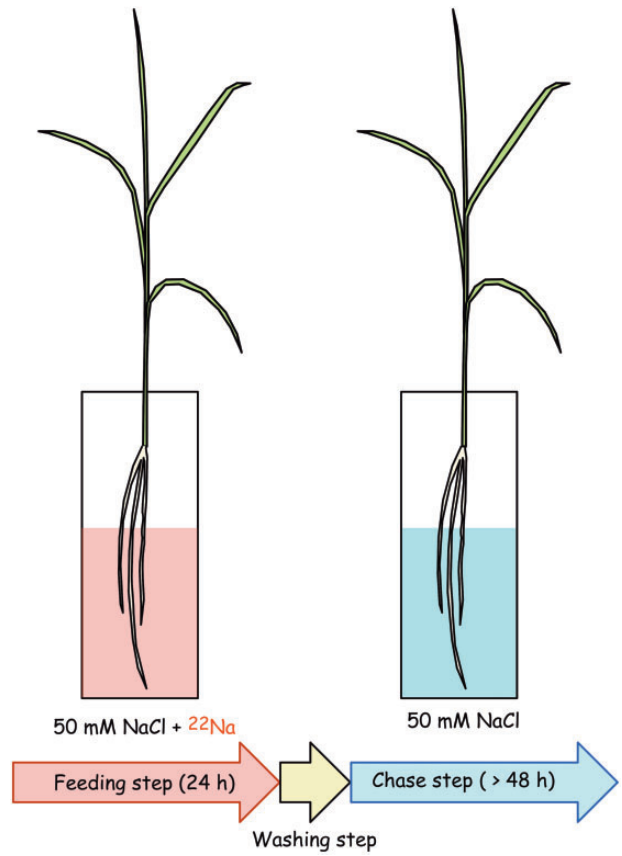

Fig. 1 Experimental set-up. At the feeding step, common reed and rice plants were incubated in a nutrient solution containing 50 mM NaCl and a trace level of radioactive ^{22}Na for 24 h. At the chase step, the original solution was replaced with a fresh one containing 50 mM NaCl but no ^{22}Na, in which the test plants were incubated for >48 h. All settings were placed on the focal plane of the PETIS, and dynamic images of ^{22}Na in plants were acquired.

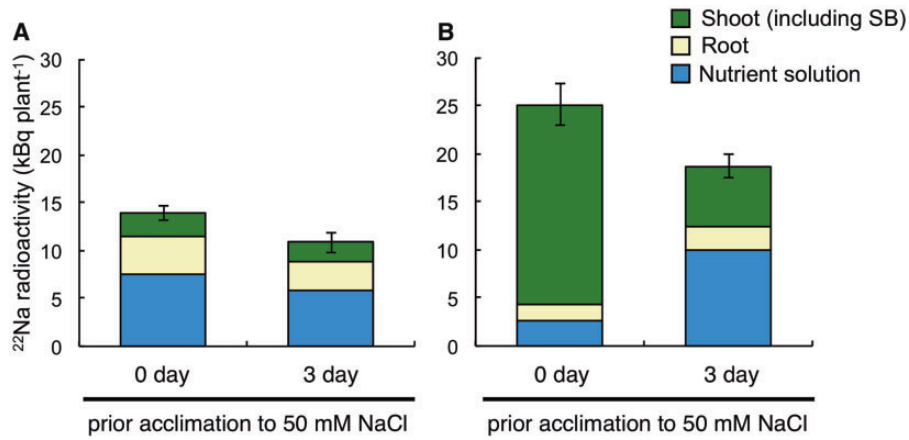

Fig. 2 Total amount of ^{22}Na absorbed by (A), common reed and (B) rice at the feeding step. At the end of the PETIS experiments, radioactivity of shoots including the shoot base, roots and nutrient solutions was measured. '0 day' indicates the case where ^{22}Na and 50 mM NaCl were supplied simultaneously. '3 day' indicates the case where ^{22}Na was supplied 3 d after 50 mM NaCl. The total amount of ^{22}Na was not significantly different between the two cases (Student's *t*-test) in both species. Values are means ± SEM of three plants.

Fig. 3 shows serial PETIS images of ^{22}Na movement in common reed and rice plants at the feeding and chase step. At the feeding step, absorbed ^{22}Na moved upwards in the roots and then strongly accumulated in the shoot base in both species (**Fig. 3B, E**). Little or no movement of ^{22}Na beyond the shoot base region was observed in common reed plants (**Fig. 3B**). In contrast, movement into and accumulation of ^{22}Na in the leaf blades were observed in rice (**Fig. 3E**). There were no obvious changes in the distribution of ^{22}Na during the chase step in the serial PETIS images for either of the two species (**Fig. 3C, F**); therefore, we performed detailed quantitative analysis of the image data.

Quantitative analysis of the longitudinal movement of ^{22}Na within root and shoot

The longitudinal movement of Na^+ in the chase step was evaluated (**Fig. 4**). First, a series of small regions of interest (ROIs) were set every 1.1 cm on the images along the plant's longitudinal axis. Then time–activity curves (i.e. the time courses of ^{22}Na amounts in the respective ROIs) were generated. ^{22}Na increased in some ROIs but decreased in others. The overall rates (per hour) of increase or decrease of radioactivity were calculated for each ROI from the time–activity curves at two time windows (0–9 h and 9–18 h). The calculated rates were standardized by dividing with the total amount of ^{22}Na absorption and then plotted against the ROIs. Individual plots of 12 tested plants are shown in **Supplementary Fig. S2**, and integrated plots per species are shown in **Fig. 5**. In these plots, the presence of a negative and a positive value in two neighboring ROIs in the same time window strongly suggests ^{22}Na movement from the former to the latter position.

In common reed (**Fig. 5A**), ^{22}Na decreased strongly directly below the shoot base (SB) (positions −04 to −01), during the initial 9 h (blue line). A steep increase in ^{22}Na was observed in the distal root region (positions −06 and −05) within the same time window (blue line). Interindividual variance was large, and the behavior of ^{22}Na accumulation in the SB was inconsistent (blue line). Between 9 and 18 h, ^{22}Na decreased in almost all regions of the root (positions −06 to 01) and the SB (red line). However, no increase in ^{22}Na was found in the upper shoot region above the SB (positions + 01 to + 08) in either time window (blue and red lines). Taken together, these data demonstrated that ^{22}Na in the roots of common reed was partially transported downwards and excluded from the field of view, but was never transported to the upper shoot above the SB in the chase step.

In rice (**Fig. 5B**), ^{22}Na decreased strongly in the basal root region, directly below the SB (positions −04 to −02) during the initial 9 h. ^{22}Na increased steeply in the SB and steadily in the upper shoot regions (positions + 01 to + 06) (blue line). However, no clear increase was observed in the distal root region (positions −06 to −05) within the same time window (blue line). Between 9 and 18 h, ^{22}Na moderately decreased in all root regions (positions −06 to −01) and increased in the upper shoot regions (positions + 01 to + 06) (red line). No obvious differences were found in the pattern of absorption and partitioning of ^{22}Na between plants with or without a 3 d acclimation pre-treatment with 50 mM NaCl (**Supplementary Fig. S2**). Taken together, these data demonstrated that in rice ^{22}Na moved mainly upwards, from the root to the upper shoot above the SB, in the chase step.

Estimation of velocity of downward movement of ^{22}Na in common reed

The time–activity curves from ROIs set in the roots below the shoot base were analyzed in a common reed plant, and **Fig. 6** shows representative results. The amount of ^{22}Na at positions −04, −05, −06 and −07 (**Fig. 6A**) peaked at 5, 7, 9 and 11 h, respectively, after the beginning of the chase step (**Fig. 6B**). The velocity of downward signal propagation was estimated at approximately 0.5 cm h^{-1}. Similar signal propagation patterns were observed in five out of six common reed plants that were tested (data not shown).

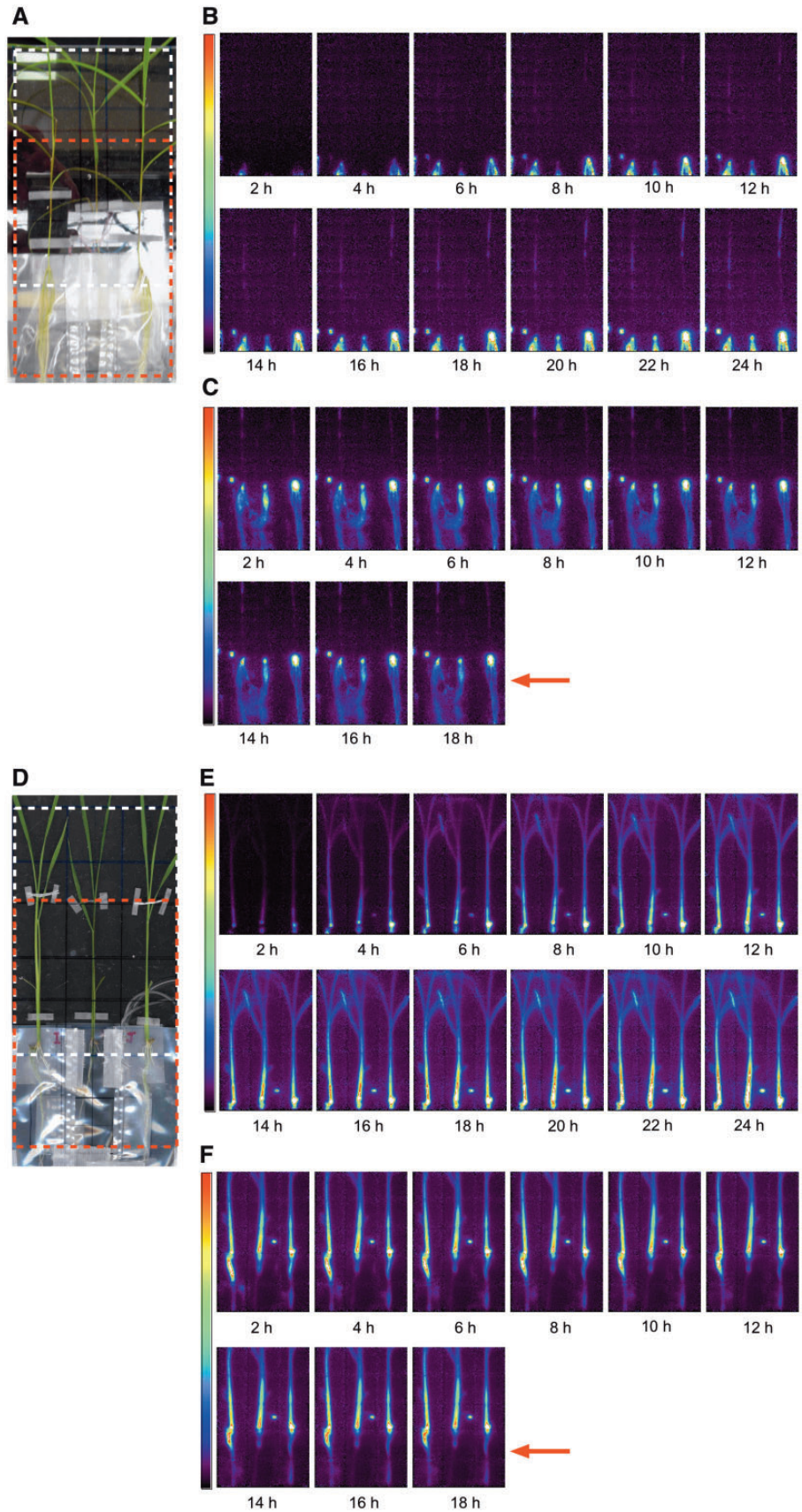

Fig. 3 Serial PETIS images showing movement of ^{22}Na in common reed (A–C) and rice plants (D–F). (A, D) Three test plants for each species were set in the field of view of the PETIS, which is indicated as dotted rectangles (white, feeding step; red, chase step). (B, E) Results of the feeding step. (C, F) Results of the chase step. Red arrows in (C) and (F) indicate the surface level of the nutrient solution.

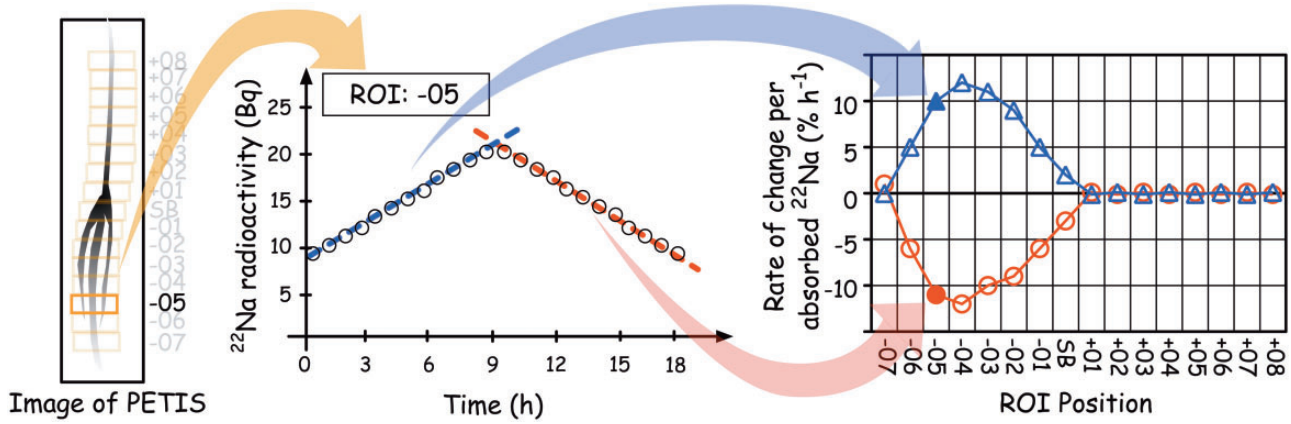

Fig. 4 Schematic representation of PETIS data analysis for ^{22}Na longitudinal movement at the chase step. Consecutive regions of interest (ROIs) were set along the plant body, and time–activity curves for the individual ROIs were generated. The overall rate of increase or decrease of ^{22}Na in respective ROIs was estimated by linear regression for 0–9 h and 9–18 h time windows. Then, the rates were normalized by the amounts of ^{22}Na absorbed by individual plants, and finally the values were plotted.

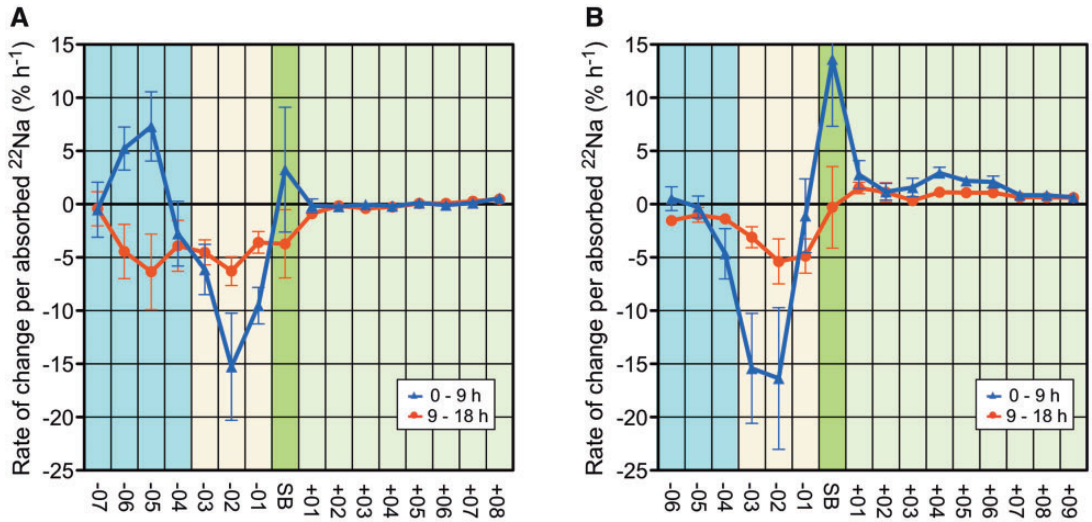

Fig. 5 Analysis of the longitudinal movement of ^{22}Na within roots and shoots of common reed (A) and rice (B). Rates of changes in ^{22}Na amounts during 0–9 h (blue lines) and 9–18 h (red lines) were plotted against the positions of ROIs. Positions −07 to −04 (pale blue) correspond to the root area submerged in the nutrient solution, −03 to −01 (pale yellow) to the root region above the surface level of the solution, and over +01 (pale green) to the upper shoot. Values are means ± SEM of six plants.

Discussion

In this study, the directions of Na^+ transport inside the plant were analyzed by using ^{22}Na and PETIS to elucidate the mechanisms of the effective exclusion of Na^+ in common reed. Na^+ movement as observed in this study was summarized in **Fig. 7**. Previous studies suggested that root to shoot (above the SB) transport of Na^+, but not soil to root absorption, is particularly limited in common reed (Matsushita and Matoh 1991, Kanai et al. 2007). In this study, the almost complete absence of Na^+ transport to the upper shoot above the SB, despite its strong accumulation in the SB, was clearly visualized by using ^{22}Na in common reed (**Fig. 3B, C**). In contrast, ^{22}Na continuously accumulated, not only in the SB, but also in the upper shoot of rice plants during the feeding step (**Fig. 3E**). This upward movement in rice continued during the chase step, even after the ^{22}Na content in the root began to decrease (**Fig. 5B**), suggesting that the root to shoot transport of Na^+ is hardly limited in rice. It should also be mentioned that the prior acclimation of the rice to 50 mM NaCl for 3 d partly suppressed the allocation of ^{22}Na to the shoot (including the SB) and enhanced excretion into the nutrient solution (**Fig. 2B**), although no obvious downward exclusion of ^{22}Na to the distal root regions in rice was detected in the PETIS experiment (**Supplementary Fig. S2**). The results from common reed raised a pivotal question: what is the mechanism that enables the complete blockage of ^{22}Na transport at the SB in common reed (**Fig. 3B**), even though there should be continuous transpiration streams with no physical barrier in xylem vessels between the root and

shoot? A previous report suggested that Na^+ is unloaded from the xylem (Kanai et al. 2007); therefore, it could be reasonable to suggest that unloading is sufficiently strong in the SB or the lower part of the root. If so, the questions that arise are: (i) where does the unloading take place; and (ii) where does the retrieved Na^+ go? Under constant 50 mM NaCl conditions, the plant must continuously excrete absorbed Na^+ in order to maintain equilibrium in the system.

Changes in ^{22}Na content during the chase step were quantitatively analyzed in continuous small sections of the root, the SB and the upper shoot to reveal the sites of Na^+ retrieval and possible subsequent longitudinal transport. In this experimental setting, the longitudinal movement of ^{22}Na from one region to another in the plant body was concluded from the decrease in ^{22}Na in the former and its simultaneous increase in the latter. **Fig. 5A** shows that in common reed ^{22}Na moved from the basal root region, 0–4.4 cm below the SB (positions −04 to −01), to the distal region (positions −06 to −05) during the initial 9 h of the chase step. Moreover, total ^{22}Na in the entire root began to decrease after 9 h, but never moved to the upper shoot above the SB (positions +01 to +08) throughout the chase step. This indicated that ^{22}Na in the root was continuously transported from the basal to the distal region. Therefore, our answer to question (i) is that Na^+ retrieval is active in the SB and the root, at least several centimeters over the basal region.

Regarding question (ii), our data in this study directly demonstrated that about half of the ^{22}Na absorbed by common reed was released to the nutrient solution during the chase step (**Fig. 2A**). There was a constitutive basal to distal transport of ^{22}Na in the root of common reed under the constant presence of Na^+ in the nutrient solution (**Fig. 5A**). The site of Na^+ excretion is still unclear, but we consider it may exist in the younger zone near the root tip, where the aerenchyma ends. Common reed has a well-developed aerenchyma that supplies air to the mature zone of the root, and thus the cortex, which lies between the stele and the epidermis, is poorly developed (**Supplementary Fig. S3A**); therefore, it seems inefficient to excrete Na^+ radially beyond such empty space from the stele. In the younger zone near the root tip, the space between the stele and the epidermis is filled with well-developed tissue (**Supplementary Fig. S3B**). Fritz and Ehwald (2013) showed that the fine lateral roots of culm-borne adventitious roots also lack developed aerenchyma in common reed. These authors suggested the existence of a radial flux of recycled Na^+ through the symplastic connection from the sieve elements to the epidermis, and Na^+ excretion to the external saline medium by active efflux in the fine lateral roots. Based on our data and this information, we assume that the longitudinal movement of Na^+ to the root tip may support Na^+ excretion from the seminal roots in common reed.

The velocity of downward Na^+ exclusion was estimated at 0.5 cm h^{-1} from the signal propagation velocity in the time–activity curves (**Fig. 6B**). The basal to distal direction of the long-distance transport in root suggested that it was driven by the phloem; however, the velocity value was considerably lower than previous estimations, calculated from the phloem transport of photoassimilates [41 ± 7 cm h^{-1} (mean ± SE, $n = 6$)

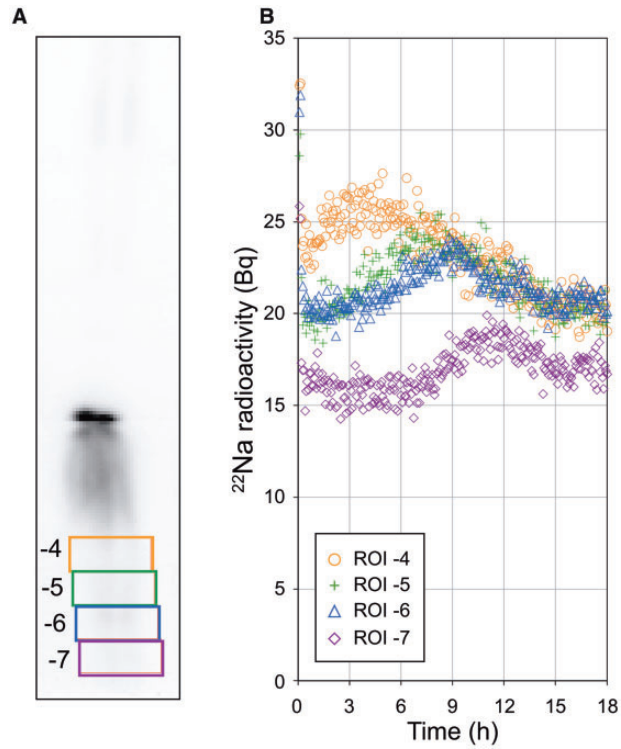

Fig. 6 Sequential propagation of ^{22}Na signal across neighboring ROIs in common reed. (A) Position of ROIs. (B) Time courses of the ^{22}Na signal in the respective ROIs.

in common reed roots (unpublished data); 18–36 cm h^{-1} in soybean roots (Fujikake et al. 2003); and phloem transport velocity (10–100 cm h^{-1}) reported as general transport velocity in the phloem (Marschner 1995)]. Our results are not consistent with those of other studies, probably because Na^+ ions can be easily unloaded from the phloem to the surrounding tissues and reloaded back into the phloem; therefore, downward exclusion of $^{22}Na^+$ may take longer than the bulk flow. Multiple unloading and reloading events may occur before individual Na^+ ions reach the excretion site in the younger zone, near the root tips. Low velocities of solute ions compared with those of assumed mass flow have also been noticed for the upward transport of cadmium in rice and of manganese in barley (Fujimaki et al. 2010).

Elucidating the molecular mechanisms of membrane transport involved in Na^+ absorption, retrieval from the xylem, unloading and reloading in the phloem, and excretion to the soil will be the next challenge. To the best of our knowledge, only two reports have described the function of transporters identified to transport Na^+ or K^+ in common reed (Takahashi et al. 2007, Takahashi et al. 2009). PhaNHA1 from common reed, a homolog of AtSOS1 that regulates the Na^+ concentration in the xylem of Arabidopsis (Shi et al. 2003), was localized in the plasma membrane of yeast and exported Na^+ from yeast cells (Takahashi et al. 2009). However, its expression site in root tissue and its contribution to Na^+ transport in roots are still unknown. PhaHKT1 from common reed is a homolog of gramineous-specific class II HKT OsHKT2;1 (Platten et al.

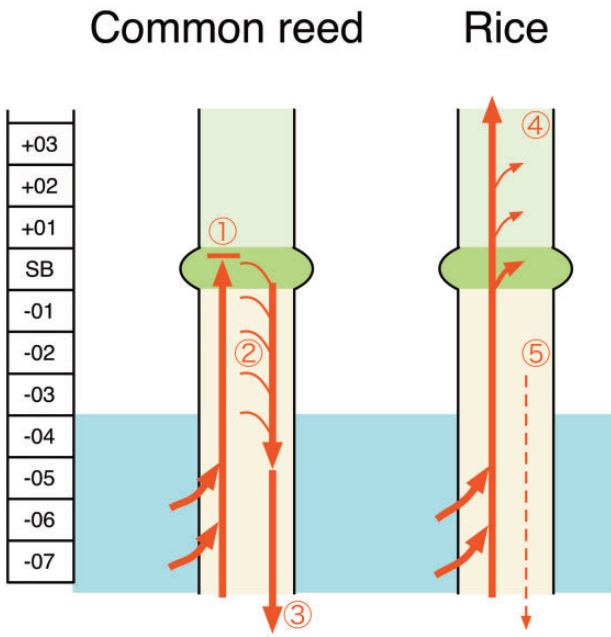

Fig. 7 Summary of Na^+ movement in common reed and rice. In common reed, (1) Na^+ was absorbed in the root part, but transport to the upper shoot above the shoot base (SB) was almost completely inhibited. (2) Na^+ retrieval was active in the SB and the basal root region. (3) Na^+ in the root was continuously transported from the basal to the distal region. In rice, (4) Na^+ was absorbed in the root part, and continuously transported to and accumulated in the SB and the upper shoot region. (5) The enhancement of Na^+ excretion into the nutrient solution by the prior acclimation to 50 mM NaCl was suggested, but no obvious downward exclusion of Na^+ in the root was detected.

2006), which contributes to K^+ homeostasis as suggested by experiments on yeast cells (Takahashi et al. 2007). A homolog of gramineous class I HKT, OsHKT1;5, which retrieves Na^+ from the xylem, has not yet reported in common reed (Ren et al. 2005, Sunarpi et al. 2005, Huang et al. 2008, Munns et al. 2012). The function and spatial expression pattern of these molecules in common reed should be revealed by further research.

Materials and Methods

Plant materials and growth conditions

Plants were cultivated in a glasshouse at a constant temperature of 24 ± 2°C under natural light (10–11 h light period). Seeds of common reed collected in Hokkaido Prefecture (Japan) were purchased from Snow Brand Seed Co., Ltd. Seeds were germinated on gauze floating on tap water in a 5 liter plastic container. Once the seedlings had reached a height of 1–2 cm, they were transferred to a half-strength nutrient solution (described below) and, once they had reached a height of 10 cm, they were transferred to a full-strength nutrient solution [1 mM $(NH_4)_2SO_4$, 0.5 mM KCl, 0.25 mM K_2HPO_4, 0.5 mM $CaCl_2$, 0.5 mM $MgCl_2$, 90 μM Fe-EDTA, 46 μM H_3BO_3, 9.2 μM $MnCl_2$, 0.32 μM $CuSO_4$, 0.77 μM $ZnSO_4$ and 0.08 μM $(NH_4)_6Mo_7O_{24}$]. Rice seeds (cv. Nipponbare) were germinated on wet paper, and the seedlings were grown in the half-strength nutrient solution. Once the first true leaf had expanded, the seedlings were transferred to the full-strength nutrient solution. For both species, the nutrient solution was renewed every 3 d, and the pH was adjusted to 6.0 with 0.2 M HCl. Six individuals of each species (20–25 cm in height) were used for experiments.

Tracer experiments

Experimental conditions. To evaluate Na^+ dynamics at steady state, the total Na^+ concentration in the nutrient solution was kept at 50 mM throughout the experiment. For three plants, ^{22}Na was fed at the same time as the nutrient solution containing non-radioactive 50 mM NaCl. For the other three individuals, ^{22}Na was applied 3 d later in order to examine possible effects of acclimation. All experiments were performed in a growth chamber with controlled conditions under continuous light at a photosynthetic photon flux density of 65 μmol s^{-1} m^{-2}) at 25°C and 65% relative humidity. Three plants were used in each imaging experiment. Plants were placed at the midplane between the two opposing detector heads of the PETIS apparatus installed in the growth chamber. The roots were placed in a plastic bag containing the nutrient solution. Air bubbles were gently supplied from the bottom of the bag throughout the experiment to maintain solution uniformity by mixing. The surface level of the solution was kept at the position indicated in **Fig. 3C, F** (below the bottom of the field of view at the feeding step) during the whole experiment by a siphon system supplying the nutrient solution without ^{22}Na. Lead blocks were placed around the bags for shielding γ-rays emitted from ^{22}Na in the solution.

Feeding step. The positions of the detector heads were adjusted so that the shoot parts were located within the field of view of PETIS (**Fig. 3A, D**, white dotted-line rectangles). Nutrient solution (10–15 ml per plant) containing 46.5 kBq ml^{-1} ^{22}Na (as NaCl; PerkinElmer Life and Analytical Sciences, Inc.) was injected into the plastic bag, instead of the non-radioactive solution. The molarity of ^{22}Na in the solution was 9 nM, relatively negligible compared with the total Na concentration. The PETIS imaging was started simultaneously with ^{22}Na injection and continued for 24 h (this period was defined as the feeding step)[0]. Each static image of ^{22}Na distribution was constructed for 4 min, and a total of 360 serial images were recorded on the computer.

Washing step. After the feeding step, the labeling solution in the plastic bag was collected and replaced with ice-cold 10 mM $CaCl_2$; the roots were incubated for 2 min to remove extra ^{22}Na from the root apoplast. This procedure was performed twice. The roots were rinsed twice with the nutrient solution containing 50 mM NaCl to remove excess Ca^{2+}.

Chase step. After the washing step, the positions of the detector heads were readjusted, so that the root parts were located within the field of view of PETIS (**Fig. 3A, D**, red dotted-line rectangles). The solution in the plastic bag was replaced with fresh nutrient solution containing 50 mM NaCl but no ^{22}Na. The PETIS imaging was performed for at least 48 h, although data for the first 18 h only were analyzed and presented in this paper. Each static image of ^{22}Na distribution was constructed for 4 min and at least 720 serial images were recorded in total on the computer. The solution was renewed at 20 h (common reed) or at 24 h (rice).

Sampling. All the culture solutions applied to the test plants during the chase step were collected. The whole shoot and the whole root parts were separately sampled after the chase step. The radioactivity of these samples was measured with a gamma well counter (NDW-351, Aloka).

PETIS apparatuses and imaging principles

An ^{22}Na atom emits a positron as a result of β^+ decay. The positron immediately collides with an electron in the plant tissue, and the resultant annihilation event produces an emission of two 511 keV of γ-rays traveling in 180° opposite directions. The PETIS apparatus (a modified PPIS-4800 model; Hamamatsu Photonics) has two opposing planar detector heads consisting of arrays of scintillators coupled with photomultipliers, and detects annihilation γ-rays with spatial and temporal information of the incident point (Uchida et al. 2004). Because the specimens are placed at the midplane between the detector heads, the position of annihilation is determined as the midpoint between the

two scintillators that detect a pair of γ-rays at the same moment. These events are recorded on a computer to reconstruct a two-dimensional static image of radiotracer distribution in the focal plane. Hundreds of serial time course images are taken, and finally the complete set of PETIS data is obtained. In this study, all images were automatically corrected for the physical decay of ^{22}Na (half-life: 2.60 years), so any changes in the ^{22}Na signal can be discussed without considering the decrease due to physical decay. Two PETIS apparatuses were used in this study with a field of view size of 142 mm (width)×215 mm (height) and 120 mm (width)×187 mm (height). The pixel size of obtained images was 1.1 mm^2.

Analysis of PETIS data

PETIS data were analyzed using NIH ImageJ 1.45 software (http://rsb.info.nih.gov/ij/, August 16, 2012). ROIs (e.g. SB) were selected on the images, and the time courses of signal intensity in each region were generated.

Supplementary data

Supplementary data are available at PCP online.

Funding

This work was supported by the Ministry of Education, Culture, Sports, Science, and Technology, Japan [Grant-in-Aid for Scientific Research grant Nos. 18658028 and 21380049 to K.H.].

Disclosures

The authors have no conflicts of interest to declare.

References

Blom-Zandstra, M., Vogelzang, S.A. and Veen, B.W. (1998) Sodium fluxes in sweet pepper exposed to varying sodium concentrations. *J. Exp. Bot.* 49: 1863–1868.

Davenport, R.J., Muñoz-Mayor, A., Jha, D., Essah, P.A., Rus, A. and Tester, M. (2007) The Na^+transporter AtHKT1;1 controls retrieval of $Na^+$from the xylem in Arabidopsis. *Plant Cell Environ.* 30: 497–507.

Fritz, M. and Ehwald, R. (2013) Radial transport of salt and water in roots of the common reed (*Phragmites australis* Trin. ex Steudel). *Plant Cell Environ.* 36: 1860–1870.

Fujikake, H., Yamazaki, A., Ohtake, N., Sueyoshi, K., Matsuhashi, S., Ito, T. et al. (2003) Quick and reversible inhibition of soybean root nodule growth by nitrate involves a decrease in sucrose supply to nodules. *J. Exp. Bot.* 54: 1379–1388.

Fujimaki, S., Suzui, N., Ishioka, N.S., Kawachi, N., Ito, S., Chino, M. et al. (2010) Tracing cadmium from culture to spikelet: noninvasive imaging and quantitative characterization of absorption, transport, and accumulation of cadmium in an intact rice plant. *Plant Physiol.* 152: 1796–1806.

Horie, T., Hauser, F. and Schroeder, J.I. (2009) HKT transporter-mediated salinity resistance mechanisms in *Arabidopsis* and monocot crop plants. *Trends Plant Sci.* 14: 660–668.

Huang, S., Spielmeyer, W., Lagudah, E.S. and Munns, R. (2008) Comparative mapping of HKT genes in wheat, barley, and rice, key determinants of Na^+transport, and salt tolerance. *J. Exp. Bot.* 59: 927–937.

James, R.A., Davenport, R.J. and Munns, R. (2006) Physiological characterization of two genes for Na^+exclusion in durum wheat, *Nax1* and *Nax2*. *Plant Physiol.* 142: 1537–1547.

Kanai, M., Higuchi, K., Hagihara, T., Konishi, T., Ishii, T., Fujita, N. et al. (2007) Common reed produces starch granules at the shoot base in response to salt stress. *New Phytol.* 176: 572–580.

Kong, X., Luo, Z., Dong, H., Eneji, A.E. and Li, W. (2012) Effects of non-uniform root zone salinity on water use, Na^+recirculation, and $Na^+$and H^+flux in cotton. *J. Exp. Bot.* 63: 2105–2116.

Lohaus, G., Hussmann, M., Pennewiss, K., Schneider, H., Zhu, J.J. and Sattelmacher, B. (2000) Solute balance of a maize (*Zea mays* L.) source leaf as affected by salt treatment with special emphasis on phloem retranslocation and ion leaching. *J. Exp. Bot.* 51: 1721–1732.

Marschner, H. (1995) Mineral Nutrition of Higher Plants, 2nd edn. Academic Press, London.

Matsushita, N. and Matoh, T. (1991) Characterization of Na^+exclusion mechanisms of salt-tolerant reed plants in comparison with salt-sensitive rice plants. *Physiol. Plant.* 83: 170–176.

Matsushita, N. and Matoh, T. (1992) Function of the shoot base of salt-tolerant reed (*Phragmites communis* Trinius) plants for Na^+exclusion from the shoots. *Soil Sci. Plant Nutr.* 38: 565–571.

Møller, I.S. and Tester, M. (2007) Salinity tolerance of *Arabidopsis*: a good model for cereals?. *Trends Plant Sci.* 12: 534–540.

Munns, R., James, R.A., Xu, B., Athman, A., Conn, S.J., Jordans, C. et al. (2012) Wheat grain yield on saline soils is improved by an ancestral Na^+transporter gene. *Nat. Biotechnol.* 30: 360–364.

Olías, R., Eljakaoui, Z., Li, J., de Morales, P.A., Marín-Manzano, M.C., Pardo, J.M. and Belver, A. (2009) The plasma membrane Na^+/H^+antiporter SOS1 is essential for salt tolerance in tomato and affects the partitioning of Na^+between plant organs. *Plant Cell Environ.* 32: 904–916.

Platten, J.D., Cotsaftis, O., Berthomieu, P., Bohnert, H., Davenport, R.J., Fairbairn, D.J. et al. (2006) Nomenclature for HKT transporters, key determinants of plant salinity tolerance. *Plant Cell Physiol.* 11: 372–374.

Ren, Z.H., Gao, J.P., Li, L.G., Cai, X.L., Huang, W., Chao, D.Y. et al. (2005) A rice quantitative trait locus for salt tolerance encodes a sodium transporter. *Nat. Genet.* 37: 1141–1146.

Shi, H., Lee, B., Wu, S.J. and Zhu, J.K. (2003) Overexpression of a plasma membrane Na^+/H^+antiporter gene improves salt tolerance in *Arabidopsis thaliana*. *Nat. Biotechnol.* 21: 81–85.

Sunarpi., Horie, T., Motoda, J., Kubo, M., Yang, H., Yoda, K. et al. (2005) Enhanced salt tolerance mediated by AtHKT1 transporter-induced Na^+unloading from xylem vessels to xylem parenchyma cells. *Plant J.* 44: 928–938.

Takahashi, R., Liu, S. and Takano, T. (2007) Cloning and functional comparison of a high-affinity K^+transporter gene *PhaHKT1* of salt-tolerant and salt-sensitive reed plants. *J. Exp. Bot.* 58: 4387–4395.

Takahashi, R., Liu, S. and Takano, T. (2009) Isolation and characterization of plasma membrane Na^+/H^+antiporter genes from salt-sensitive and salt-tolerant reed plants. *J. Plant Physiol.* 166: 301–309.

Uchida, H., Okamoto, T., Ohmura, T., Shimizu, K., Satoh, N., Koike, T. et al. (2004) A compact planar positron imaging system. *Nucl. Instrum. Methods Phys. Res., Sect. A* 516: 564–574.

Wolf, O., Munns, R., Tonnet, M.L. and Jeschke, W.D. (1990) Concentrations and transport of solutes in xylem and phloem along the leaf axis of NaCl-treated. *Hordeum vulgare*. *J. Exp. Bot.* 41: 1133–1141.